Voxelized Breast Phantoms for Dosimetry in Mammography

R. M. Tucciariello[1,2] [a], P. Barca [1] [b], D. Del Sarto[1,2] [c], R. Lamastra[1,2], G. Mettivier[3,4] [d],
A. Retico[2] [e], P. Russo[3,4] [f], A. Sarno[3] [g], A. C. Traino[5] [h] and M. E. Fantacci[1,2] [i]

[1]*Department of Physics, University of Pisa, Pisa, Italy*
[2]*INFN, Pisa Section, Pisa, Italy*
[3]*INFN, Napoli Section, Napoli, Italy*
[4]*Università di Napoli Federico II, Dipartimento di Fisica "Ettore Pancini", Napoli, Italy*
[5]*Unit of Medical Physics, Pisa University Hospital "Azienda Ospedaliero-Universitaria Pisana", Pisa, Italy*

Keywords: Monte Carlo Simulations, Digital Mammography, X-Ray Breast Dosimetry, Voxelized Phantoms, Heterogeneous Breast Phantoms, GEANT4.

Abstract: X-ray breast imaging techniques are an essential part of breast cancer screening programs and their improvements lead to gain in performance and accuracy. Radiation dose estimate and control play an important role in digital mammography and digital breast tomosynthesis investigations, since the risk of radioinduced cancer to the gland must be contained and dose delivered to the gland must be declared in the medical report. The actual dosimetric protocols suggest the assessment of radiation dose by means of Monte Carlo calculation on digital breast phantoms, providing the assumption of the homogeneous mixture of glandular and adipose tissues within the breast organ, leading to a drastic approximation. In line with the trend of other research groups, with the aim of improving the Monte Carlo model, in the current work a new heterogeneous digital breast model is proposed, involving a voxelized approach and disengaging from the concept of homogeneous phantom. The proposed model is based on new findings in the literature and after a validation process, the model is adopted to evaluate mean glandular dose discrepancies with the traditional model which is adopted in clinic for decades.

1 INTRODUCTION

Worldwide, breast cancer is the most commonly diagnosed cancer in female subjects, accounting about 2.1 million newly diagnosed breast cancer, with 1 in 4 cancer cases among women, and the leading cause of cancer death, followed by colorectal and lung cancer for incidence, and vice versa for mortality (Yuuhaa et al., 2018). In 2018, among European women, breast cancer was by far the most frequently diagnosed neoplasm (522,500 , 28.2% of the total), followed by colorectal (228,000 , 12.3%), lung (158,000 , 8.5%) and corpus uteri (122,000 , 6.6%) cancers (Ferlay et al., 2018).

As suggested by the World Health Organization, early detection is critical to improve breast cancer outcomes and survival, made possible with screening procedures consisting in testing women to identify cancers before any symptom appears. This may lead to tumour early detection, allowing greater

[a] https://orcid.org/0000-0001-9600-4177
[b] https://orcid.org/0000-0001-9692-0730
[c] https://orcid.org/0000-0003-3293-1005
[d] https://orcid.org/0000-0001-6606-4304
[e] https://orcid.org/0000-0001-5135-4472
[f] https://orcid.org/0000-0001-9409-0008
[g] https://orcid.org/0000-0002-3034-7166
[h] https://orcid.org/0000-0003-3521-6293
[i] https://orcid.org/0000-0003-2130-4372

possibilities for medical treatment and reducing the mortality rate. Since last decades, the principal technique adopted for breast cancer screening programs is the Digital Mammography (DM), an X-ray imaging technique consisting in acquiring two digital images, a cranio-caudal and a medio-lateral view; since 2011 when it was introduced in the clinical routine, the new technique Digital Breast Tomosynthesis (DBT) (Sechopoulos, 2013a, 2013b) supports or might even replace DM, because it allows to reduce the tissue superimposition effect, making it easier for radiologists to distinguish normal from cancerous tissues.

Since breast imaging techniques involve ionizing radiation, radiation dosimetry must be accurately assessed the glandular tissue is considered as the target tissue for radiation damage. Radioinduced cancer risk estimates are performed by using the *Average Glandular Dose* (AGD) metric as defined in UK and EU dosimetry protocol (Van Engen et al., 2018) or also referred as *Mean Glandular Dose* (MGD). It should be stressed that breast screening procedures involve low-dose radiation and the carcinogenic risk is small with a very favourable trade-off of the potential beneficial effects of screening with respect to the calculated risk of induced cancer (Pauwels et al., 2016).

For both DM and DBT, dosimetry is performed by using Monte Carlo simulations (Wu et al. 1994; Dance and Sechopoulos 2016; Sarno et al. 2018; Tucciariello et al. 2020) which involve models of the anatomy of the breast (digital phantoms) with a homogeneous mixture of glandular and adipose tissues, surrounded by a skin envelope. This methodology does not consider real heterogeneous glandular distribution within the breast and the assumption of the homogeneous compound is very drastic (Sarno et al. 2018). Nevertheless, the advent of the fully 3D quantitative technique of Breast Computed Tomography (bCT) (Sarno, Mettivier, and Russo 2015), helped to better characterize the breast anatomy. On the basis of the results provided by Huang and Hernandez (Hernandez et al. 2015; Huang et al. 2011) which involved real bCT investigations on patients, in this work a new voxelized phantom model, which takes into account the heterogeneous distribution of the gland, has been created to be adopted for improving the accuracy of the Monte Carlo (MC) simulations in dosimetry for DM and DBT.

In view of the publication of the Task Group 282 of the AAPM in collaboration with EFOMP for the development of a new universal breast dosimetry, the purpose of this work is to propose a new heterogeneous breast model which is more representative of the real breast anatomies with respect to the adoption of an homogeneous breast model. Indeed, a simple glandular distribution model is presented and the influence of this methodology on dose estimates will be evaluated by comparing MGD values with those of the homogeneous model. Sarno et al. (2018) followed an alternative approach in which a dataset of real investigations is involved for dosimetry purposes and patient-specific dose estimates are performed. It has to be said that this represents a complex and time-consuming approach, which takes in consideration one-by-one women breast, while the proposed methodology in this work adopts the average glandular distribution among women.

2 MATERIALS AND METHODS

The radiation glandular dose cannot be assessed experimentally and the use of Monte Carlo simulations (MC) is required. MGD estimates are performed by using dedicated conversion coefficients from the incident Air Kerma (K_{air}, mGy) to MGD values (mGy). In this work, the formalism provided by Wu (Wu et al., 1994) and extended by Boone (Boone, 1999) is adopted to estimate the MGD values (eq. 1).

$$MGD\ [mGy] = DgN \cdot K_{air} \qquad (1)$$

where DgN is the normalized glandular dose coefficient (mGy/mGy).

In MC calculations, the rationale is to perform simulations of the X-ray beam by tracing every simulated photon over its track, from the radiation source, towards the breast and to register energy deposits in the volume (or mass) of interest. The MC method produces the DgN coefficients through the calculation of the MGD (which cannot be estimated experimentally) and K_{air} (measurable quantity). The clinical practice uses DgN numbers for converting the measured K_{air} at the entrance surface of the breast to the estimated MGD values (Sarno et al. 2019).

2.1 The Proposed Model

Using the GEANT4 simulation toolkit (Agostinelli et al., 2003), following previous studies (Sarno et al. 2017; 2018; 2019) the setup for simulations has been replicated and reported in Figure 1. The scoring volume for dose deposit is showed in pink colour and the skin envelope is considered as a shielding layer of 1.45 mm thick (Huang et al., 2008) not involved for

the dose computation. Adipose and glandular tissues was replicated in the simulation setup by using the elemental composition (Hammerstein et al., 1979), reported in Table 1. The methodology adopted in this work employs a new phantom model which disengages from the traditional method of estimating the mean glandular dose; indeed, the well-known *G-factor* is adopted for "correcting" the dose deposit in the homogeneous phantom (Boone 1999, 2002; Nosratieh et al. 2015; Sarno et al. 2018; Sarno, Mettivier, and Russo 2017; Tucciariello et al. 2019). The traditional methodology of estimating MGD values for homogeneous phantoms has been deeply investigated in literature and is not the intent of this paper.

Table 1: Elemental composition and density for glandular and adipose tissues as implemented in the MC code.

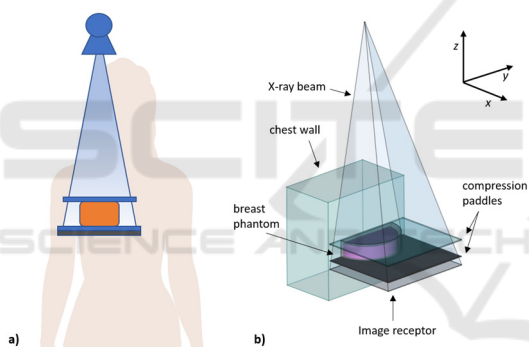| Tissue	H	C	N	O	P	density (g/cm^3)
glandular	0.102	0.184	0.032	0.677	0.005	1.04
adipose	0.112	0.619	0.017	0.251	0.001	0.93
skin	0.098	0.178	0.050	0.667	0.007	1.09

Figure 1: a) Schematic drawing of the cranio-caudal view irradiation geometry; b) scheme of the adopted simulation geometry.

To move towards a heterogeneous approach, the volume inside the breast tissue has to be divided in voxels by using a voxel grid, inside which either adipose or glandular tissues can be included, with voxel dimension of 1×1×1 mm^3. Since cubic voxels have to be fixed inside a non-cubic volume (semi-cylindrical cross section), some space uninvolved by glandular tissue occurs, mainly between the breast tissue and the skin interface on the rounded side of the phantom, while on the chest wall side the border of the voxels grid perfectly overlaps with the border of the breast tissue. Despite uninvolved space reduces

while decreasing voxels dimensions, computational times and memory required have to be considered and optimized. For purely investigative purposes, in the presented model a voxel dimension of 1×1×1 mm^3 is used, leading to a grid generation time of few seconds to generate the whole voxel grid and only about 100 MB of RAM are required for the digital phantom initialization. Nevertheless, uninvolved volume is occupied by adipose material, which surely surrounds the breast gland on the interface with the skin layer (Huang et al. 2011) and this geometrical approximation can be negligible.

Huang and Hernandez (Hernandez et al. 2015; Huang et al. 2011) characterized the glandular tissue within the breast, providing a metric able to reproduce it. bCT investigations performed over patients let to explore different breast anatomies (various cup sizes and glandularities[1]) and a representative model has been chosen for simulations.

In order to create a representative phantom model, comparable with the homogeneous one adopted previously, for which dose estimates are available in the literature, the semi-cylindrical cross section has been maintained. The use of a single gaussian distribution, with no right-left displacement (as showed by Huang) is considered appropriate in order to replace a representative phantom for both right and left women breasts, and an average value of 0.34 for the FWHM provided by Hernandez has been adopted. Equation (2) shows the distribution for glandular voxels within the breast over the directions y and z, represented by d (see Figure 2), for a given compressed breast thickness l, μ_d the centers of the distributions and σ_d the standard deviations in both directions (eq. 3).

$$G(d, \sigma_d) = \frac{1}{\sqrt{2\pi\sigma_d^2}} \, e^{-\frac{(d-\mu_d)^2}{2\sigma_d^2}} \qquad (2)$$

$$\sigma_d = \frac{FWHM}{2.35} \cdot l \qquad (3)$$

The choice of the material for each voxel is performed by using a random approach, following the distribution criteria adopted for the glandular tissue. The assignment of glandular rather than adipose material for each voxel is carried out by using $G(d, \sigma_d)$. The product $G(y, \sigma_y) \cdot G(z, \sigma_z)$ provides the probability that a certain voxel in position (y,z) is composed by glandular material depending of its position in the breast volume. The randomness with

---

[1] The term *glandularity* indicates the percentage of glandular tissue respect to the adipose tissue, sometimes referred as *breast density*.

which voxels are effectively fulfilled or not with glandular material is provided by the uniform probability distribution in the interval [0,1] produced by the GEANT4 random number generator. The amount of glandular voxels can be tuned in the MC code to reproduce different breast densities.
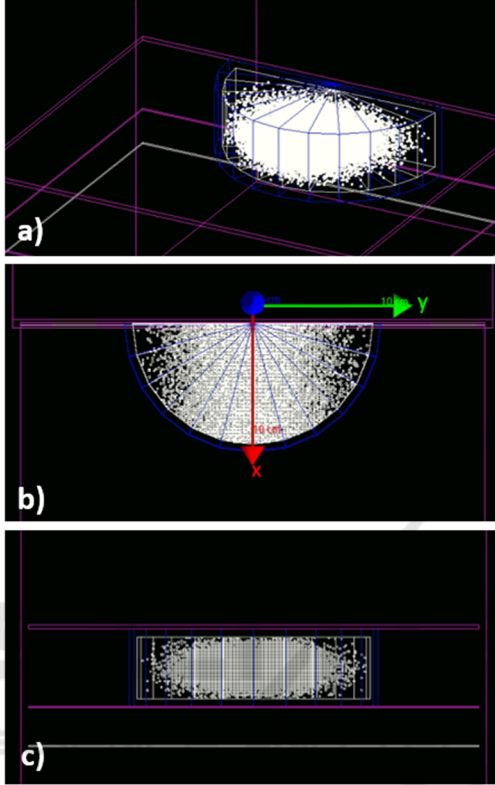

Figure 2: a) perspective, b) top and c) front views of the proposed voxelized breast phantom. Glandular distributions evolve in y and z directions with gaussian distributions, while in x direction with a constant distribution. The voxel grid concerns the whole breast tissue volume (white semi-cylinder) and for an easy display purpose only glandular voxels are showed, while the remaining part has to be considered filled with adipose tissue.

2.2 Model Validation

A fundamental aspect of MC calculations is the validation process. The MC code adopted derives from a previously validated MC code for homogeneous breast phantoms. The validation process consisted in comparisons against literature (Dance, Young, and Van Engen 2011; Sechopoulos et al. 2014; AAPM TG 2015) and experimental measurements by using radiochromic films.

Since in this work the code has been upgraded to produce voxelized heterogeneous breast phantoms, any consistent change in the model adopted should be

confirmed by some kind of verification. For validation purposes of the voxelized methodology, the phantom grid has been set using the uniform probability distribution for assigning either glandular or adipose tissues for each voxel. The rationale is to compare MGD simulations results for the grid phantom, with voxels randomly filled replicating a uniform distribution of gland, with those of the homogeneous phantom with the same breast density. Three compression thicknesses of 3, 5 and 7 cm, and five glandularities of 1%, 14.3%, 25%, 50% and 75% have been replicated. For each model three spectra have been involved for investigating different beam qualities. In this case, MGD estimates do not involve the usual relation provided by (Boone, 1999; Nosratieh et al., 2015; A. Sarno, Mettivier, Di Lillo, Tucciariello, et al., 2018), but is directly obtained by scoring the energy deposited E_i in all the n glandular voxels with mass m_{vox} due to the X-ray beam (eq. 4)

$$MGD = \sum_{i=1}^{n} \frac{E_i}{n \cdot m_{vox}} \qquad (4)$$

2.3 Dose Estimates

Glandular dose estimates dependencies using homogeneous phantoms have already been investigated by many authors (Dance and Sechopoulos 2016; Sarno et al. 2018, 2019; Tucciariello et al. 2020; Tucciariello et al. 2019) and are not within the intents of this work, but no evidences have been published in literature about the dependence of dose estimates with respect to the breast density obtained with heterogeneous glandular distribution within the breast. In order to quantify discrepancies between the two methods, simulations have been performed with both homogeneous and heterogeneous models, for three compressed thicknesses of 3, 5 and 7 cm, exposed respectively to W/Rh 26 kV, W/Rh 31 kV and W/Ag 34 kV spectra. For each breast thickness, 12 glandularities have been replicated.

3 RESULTS

3.1 Voxelized Phantom Validation

The voxelized phantom validation process regarded the comparison between MGD values obtained with the homogeneous phantom (MGD_hom) with those obtained with the voxelized phantom (MGD_vox) using the constant distribution of gland among voxels. This kind of verification, performed by choosing the same

breast density in both models, let to investigate the discrepancy produced by the voxelized model, regardless of the glandular distribution adopted. MGD discrepancies are showed in Table 2, where a maximum percentage difference of 2.3% and an average value of 1.0% confirm the success of the voxels grid phantom model. Figure 3 highlights the goodness of the fit ($R^2 \simeq 0.9995$) performed over the data obtained from simulations.

Since the creation of each heterogeneous digital breast phantom involves a Monte Carlo approach, the degree of reproducibility is questionable and one has to wonders how much a certain model will differ with the next one, with the same requested glandularity, in terms of the amount of glandular voxels effectively created and of mean glandular dose estimation. The rationale is to create multiple models with same glandularity and to verify the reproducibility capabilities of the MC code. With the same methodology, for each breast thickness of 3, 5 and 7 cm, five glandularities have been requested to be reproduced by the MC code. In addition, for each glandularity five models have been created, for a total of 75 models, each of them irradiated with W/Al spectra. In this case, between models with same glandularity required, a maximum standard deviation of 0.05% of glandularity is reached, which traduces in very low MGD discrepancies, less than 0.5%.

Table 2: Data comparison between MGD values obtained with homogeneous and voxelized phantoms for five breast densities. Percentage differences refer to the ratio (MGD_{hom} - MGD_{vox})/ $MGD_{hom} \times 100\%$.

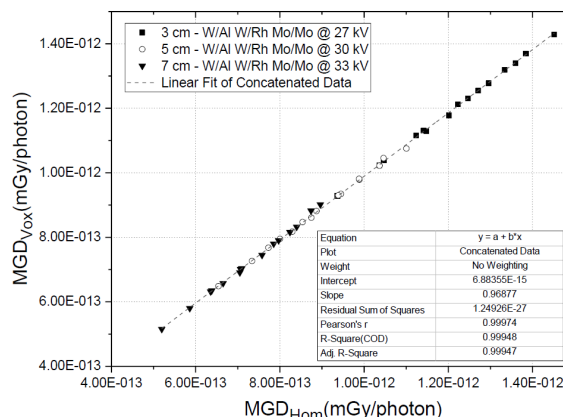|	MGD$_{vox}$ vs MGD$_{hom}$				
	1%	*14.3%*	*25%*	*50%*	*75%*
3 cm – W/Al 27kV	**1.5%**	**1.4%**	**1.3%**	**0.9%**	**0.7%**
3 cm – W/Rh 27kV	**1.6%**	**1.1%**	**1.1%**	**0.9%**	**0.7%**
3 cm – Mo/Mo 27kV	**1.3%**	**2.0%**	**1.7%**	**1.3%**	**0.9%**
5 cm – W/Al 30kV	**0.1%**	**1.1%**	**1.1%**	**0.8%**	**0.7%**
5 cm – W/Rh 30kV	**2.3%**	**1.4%**	**0.7%**	**0.7%**	**0.6%**
5 cm – Mo/Mo 30kV	**0.9%**	**1.6%**	**1.5%**	**1.0%**	**0.9%**
7 cm – W/Al 33kV	**-1.0%**	**1.0%**	**0.7%**	**0.8%**	**0.6%**
7 cm – W/Rh 33kV	**-0.6%**	**0.9%**	**0.9%**	**0.9%**	**0.6%**
7 cm – Mo/Mo 33kV	**1.7%**	**2.0%**	**1.2%**	**1.1%**	**0.8%**

Figure 3: Linear fit of MGD$_{vox}$ versus MGD$_{hom}$ in units of mGy per incident photon. Concatenated data for 3, 5 and 7 cm compressed breast thicknesses. *Origin 9.4* data analysis software.

3.2 Dose Estimates in Mammography

Once the upgraded MC code which uses the proposed phantom model has been validated, simulations over the new model can be performed and new MGD values could be investigated. As one can easily guess, the adoption of the new model can lead to new MGD values considering that the gland is mainly spread in the central part of the volume. Di Franco and colleagues (Di Franco et al., 2020) investigated the glandular dose map within patient-derived digital phantoms and highlighted a major dose distribution towards the X-ray beam incident side (see Figure 1), where however it should be mainly adipose voxels.

This kind of considerations led to treat the results showed in Figure 4a more than reasonable, where digital mammography investigations have been performed for homogeneous and heterogeneous breast models for various glandularities. Indeed, in the homogeneous phantom a greater amount of glandular tissue is in the upper layer of the breast with the respect to the heterogeneous one, and glandular dose deposit is higher, while in the heterogeneous phantom the X-ray beam undergoes an X-ray attenuation mainly due to the adipose tissues in the upper layers and dose deposit is not scored by the MC code. This effect also traduces in more discrepancies for higher breast thicknesses and lower glandularities, since glandular voxels are mainly disposed farther from the upper surface.
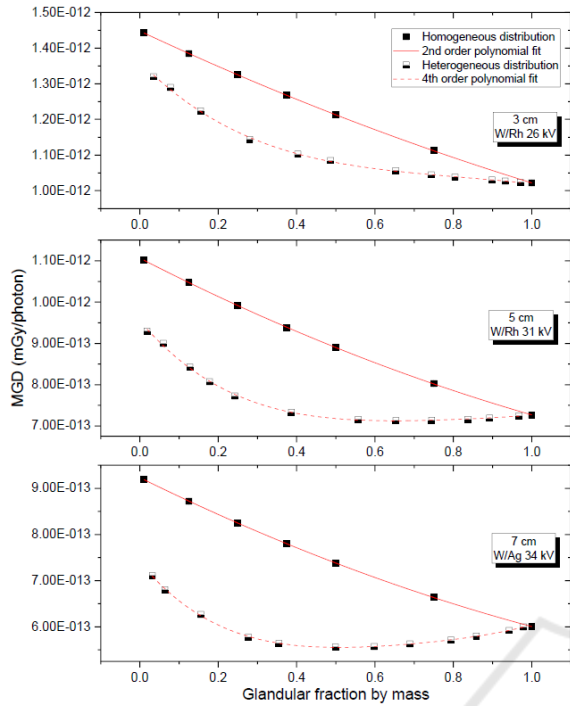
Figure 4: Mean glandular dose (mGy/photon) comparison between the homogeneous breast model and the voxelized one. Points in graphs refer to different glandularities. Simulations have been performed by using the Hologic Selenia Dimensions setup and typical irradiation settings in DM modality for breast thicknesses of 3, 5 and 7 cm.

Discrepancies between MGD_{het} and MGD_{hom} are reported in Table 3. Larger percentage variations occur for breast densities less than 50% and decrease with the increase of the breast density. It is a clear evidence that for higher glandularities voxels marked with gland tissue expand towards the border of the phantom, approaching the 100% glandularity while expanding and get closer to the homogeneous model.

As opposed to MGD coefficients for homogeneous phantoms, which trend follows a 2nd order polynomial fit respect to the breast density (Sarno et al. 2018), dose estimates for the voxelized phantom show a 4th order polynomial fit dependence against glandularity, for both low and high compressed breast thicknesses, where, moreover, for 7 cm thickness a non-monotone trend is presented and a concave curve is highlighted (Figure 4).

Discrepancies highlighted in Table 3 are in line with literature (Dance et al. 2005; Hernandez et al. 2015) and these results should be emphasized, because major variations occur for the most popular breast densities among female subjects.

Table 3: Percentage variation of dose estimates between heterogeneous and homogeneous models. $(MGD_{hom} - MGD_{het})/ MGD_{hom} \times 100\%$.

Model #	3 cm		5 cm		7 cm	
	Glandularity (normalized)	variation (%)	gland.	var. (%)	gland.	var. (%)
1	0.03	**-8.3%**	0.02	**-18.0%**	0.03	**-28.0%**
2	0.08	**-9.2%**	0.06	**-19.7%**	0.06	**-31.9%**
3	0.16	**-11.9%**	0.13	**-24.1%**	0.16	**-37.3%**
4	0.28	**-14.6%**	0.18	**-26.8%**	0.28	**-41.1%**
5	0.40	**-13.8%**	0.24	**-28.8%**	0.35	**-39.5%**
6	0.49	**-12.3%**	0.39	**-27.4%**	0.50	**-32.7%**
7	0.65	**-8.9%**	0.56	**-21.3%**	0.60	**-27.0%**
8	0.74	**-6.7%**	0.65	**-17.0%**	0.69	**-20.9%**
9	0.80	**-5.2%**	0.74	**-12.6%**	0.79	**-14.0%**
10	0.90	**-2.6%**	0.84	**-8.1%**	0.86	**-9.4%**
11	0.93	**-1.8%**	0.89	**-5.3%**	0.94	**-3.7%**
12	0.97	**-0.8%**	0.97	**-1.5%**	0.98	**-1.0%**

4 CONCLUSIONS

Since the 90's, X-ray breast dosimetry has been performed with Monte Carlo calculations by adopting the assumption of the homogenous compound of the breast tissue. Studies in literature showed a non-uniform distribution of the glandular tissue and quantitative data are available. This work was aimed to overcome the drastic approximation of the current digital breast phantom and therefore to improve Monte Carlo accuracy for dosimetry in DM and DBT. Based on findings in the literature, involving results from real bCT scans on patients, a new methodology for creating digital breast phantoms is proposed, in order to provide a more representative phantom to adopt for dose estimates; the proposed model involves a voxelized phantom with glandular voxels which follow a gaussian distribution among vertical and lateral axis. The validation phase has been conducted by comparing the current dosimetry methodology with the proposed one, showing good reliability and reproducibility of the voxelized method. Finally, MC calculations have been performed for both homogeneous and heterogeneous models in typical DM investigations, in order to quantify the discrepancy between the two phantom models; wide variations have been confirmed, mostly for low breast densities, the most common characteristic among women and a new trend curve has been found regarding the MGD values versus the glandularity. The underestimates of MGD values with the adoption of the voxelized phantom are in line with literature results.

Nevertheless, a justification for today's adoption of the old protocols based on homogeneous phantoms can be given by confirming a conservative approach of the actual method related to glandular dose. More alarming would have been if the comparison would lead to exactly opposite results. However, it must be said that the MC approach is aimed to reproduce experimental configuration with a certain degree of accuracy, and the better the methodology used, the greater the reliability. Moreover, MC calculations are particularly useful for optimizing support equipment for experimental measurements, like physical breast phantoms for quality assurance or research activities in the field of imaging (Ivanov et al. 2018; Tucciariello et al. 2020; Barca et al. 2019; Lamastra et al. 2020) and efforts in Monte Carlo calculations represent one of the right ways to go through.

ACKNOWLEDGEMENTS

REFERENCES

Agostinelli, S., Allison, J., Amako, K., Apostolakis, J., Araujo, H., Arce, P., Asai, M., Axen, D., Banerjee, S., Barrand, G., Behner, F., … Zschiesche, D. (2003). GEANT4 - A simulation toolkit. *Nuclear Instruments and Methods in Physics Research, Section A: Accelerators, Spectrometers, Detectors and Associated Equipment*, *506*(3), 250–303. https://doi.org/10.1016/S0168-9002(03)01368-8

Barca, P., Lamastra, R., Aringhieri, G., Tucciariello, R. M., Traino, A., & Fantacci, M. E. (2019). Comprehensive assessment of image quality in synthetic and digital mammography : a quantitative comparison. *Australasian Physical & Engineering Sciences in Medicine*, *Cd*. https://doi.org/10.1007/s13246-019-00816-8

Boone, J. M. (1999). Glandular breast dose for monoenergetic and high-energy x-ray beams: Monte Carlo assessment. *Radiology*, *213*(1), 23–37. https://doi.org/10.1148/radiology.213.1.r99oc3923

Boone, J. M. (2002). Normalized glandular dose (DgN) coefficients for arbitrary x-ray spectra in mammography: Computer-fit values of Monte Carlo derived data. *Medical Physics*, *29*(5), 869–875. https://doi.org/10.1118/1.1472499

Dance, D. R., Young, K. C., & Van Engen, R. E. (2011). Estimation of mean glandular dose for breast tomosynthesis: Factors for use with the UK, European and IAEA breast dosimetry protocols. *Physics in Medicine and Biology*, *56*(2), 453–471. https://doi.org/10.1088/0031-9155/56/2/011

Dance, David R., Hunt, R. A., Bakic, P. R., Maidment, A. D. A., Sandborg, M., Ullman, G., & Carlsson, G. A. (2005). Breast dosimetry using high-resolution voxel phantoms. *Radiation Protection Dosimetry*, *114*(1–3), 359–363. https://doi.org/10.1093/rpd/nch510

Dance, David R., & Sechopoulos, I. (2016). Dosimetry in x-ray-based breast imaging. *Physics in Medicine and Biology*, *61*(19), R271–R304. https://doi.org/10.1088/0031-9155/61/19/R271

Di Franco, F., Sarno, A., Mettivier, G., Hernandez, A. M., Bliznakova, K., Boone, J. M., & Russo, P. (2020). GEANT4 Monte Carlo simulations for virtual clinical trials in breast X-ray imaging: Proof of concept. *Physica Medica*, *74*(November 2019), 133–142. https://doi.org/10.1016/j.ejmp.2020.05.007

Ferlay, J., Colombet, M., Soerjomataram, I., Dyba, T., Randi, G., Bettio, M., Gavin, A., Visser, O., & Bray, F. (2018). Cancer incidence and mortality patterns in Europe: Estimates for 40 countries and 25 major cancers in 2018. In *European Journal of Cancer* (Vol. 103, pp. 356–387). Elsevier Ltd. https://doi.org/10.1016/j.ejca.2018.07.005

Hammerstein, G. R., Miller, D. W., White, D. R., Masterson, M. E., Woodard, H. Q., & Laughlin, J. S. (1979). Absorbed radiation dose in mammography. *Radiology*, *130*(2), 485–491.

Hernandez, A. M., Seibert, J. A., & Boone, J. M. (2015). Breast dose in mammography is about 30% lower when realistic heterogeneous glandular distributions are considered. *Medical Physics*, *42*(11), 6337–6348. https://doi.org/10.1118/1.4931966

Huang, S. Y., Boone, J. M., Yang, K., Kwan, A. L. C., & Packard, N. J. (2008). The effect of skin thickness determined using breast CT on mammographic dosimetry. *Medical Physics*, *35*(4), 1199–1206. https://doi.org/10.1118/1.2841938

Huang, S. Y., Boone, J. M., Yang, K., Packard, N. J., McKenney, S. E., Prionas, N. D., Lindfors, K. K., & Yaffe, M. J. (2011). The characterization of breast anatomical metrics using dedicated breast CT. *Medical Physics*, *38*(4), 2180–2191. https://doi.org/10.1118/1.3567147

Ivanov, D., Bliznakova, K., Buliev, I., Popov, P., Mettivier, G., Russo, P., Di Lillo, F., Sarno, A., Vignero, J., Bosmans, H., Bravin, A., & Bliznakov, Z. (2018). Suitability of low density materials for 3D printing of physical breast phantoms. *Physics in Medicine and Biology*, *63*(17), aad315. https://doi.org/10.1088/1361-6560/aad315

Lamastra, R., Barca, P., Bisogni, M. G., Caramella, D., Rosso, V., Tucciariello, R. M., Traino, A. C., & Fantacci, M. E. (2020). Image quality comparison between synthetic 2D mammograms obtained with 15° and 40° X-ray tube angular range: A quantitative

phantom study. *BIOIMAGING 2020 - 7th Int. Conf. Bioimaging, Proceedings; Part 13th Int. Jt. Conf. Biomed. Eng. Syst. Technol., BIOSTEC 2020, Biostec*, 184–191. https://doi.org/10.5220/0009147601840191

Nosratieh, A., Hernandez, A., Shen, S. Z., Yaffe, M. J., Seibert, J. A., & Boone, J. M. (2015). Mean glandular dose coefficients (DgN) for x-ray spectra used in contemporary breast imaging systems. *Physics in Medicine and Biology*, *60*(18), 7179–7190. https://doi.org/10.1088/0031-9155/60/18/7179

Pauwels, E. K. J., Foray, N., & Bourguignon, M. H. (2016). Breast Cancer Induced by X-Ray Mammography Screening? A Review Based on Recent Understanding of Low-Dose Radiobiology. *Medical Principles and Practice*, *25*(2), 101–109. https://doi.org/10.1159/000442442

Sarno, A., Mettivier, G., Di Lillo, F., Bliznakova, K., Sechopoulos, I., & Russo, P. (2018). Homogeneous vs. patient specific breast models for Monte Carlo evaluation of mean glandular dose in mammography. *Physica Medica*. https://doi.org/10.1016/j.ejmp.2018.04.392

Sarno, A., Mettivier, G., Di Lillo, F., Tucciariello, R. M., Bliznakova, K., & Russo, P. (2018). Normalized glandular dose coefficients in mammography, digital breast tomosynthesis and dedicated breast CT. *Physica Medica*, *55*, 142–148. https://doi.org/10.1016/j.ejmp.2018.09.002

Sarno, A., Tucciariello, R. M., Mettivier, G., di Franco, F., & Russo, P. (2019). Monte Carlo calculation of monoenergetic and polyenergetic DgN coefficients for mean glandular dose estimates in mammography using a homogeneous breast model. *Physics in Medicine and Biology*, *64*(12), 125012. https://doi.org/10.1088/1361-6560/ab253f

Sarno, Antonio, Mettivier, G., & Russo, P. (2015). Dedicated breast computed tomography: Basic aspects. *Medical Physics*, *42*(6), 2786–2804. https://doi.org/10.1118/1.4919441

Sarno, Antonio, Mettivier, G., & Russo, P. (2017). Air kerma calculation in Monte Carlo simulations for deriving normalized glandular dose coefficients in mammography. *Physics in Medicine and Biology*. https://doi.org/10.1088/1361-6560/aa7016

Sechopoulos, I. (2013a). A review of breast tomosynthesis. Part I. The image acquisition process. *Medical Physics*. https://doi.org/10.1118/1.4770279

Sechopoulos, I. (2013b). A review of breast tomosynthesis. Part II. Image reconstruction, processing and analysis, and advanced applications. *Medical Physics*. https://doi.org/10.1118/1.4770281

Sechopoulos, I., Sabol, J. M., Berglund, J., Bolch, W. E., Brateman, L., Christodoulou, E., Flynn, M., Geiser, W., Goodsitt, M., Kyle Jones, A., … Von Tiedemann, M. (2014). Radiation dosimetry in digital breast tomosynthesis: Report of AAPM Tomosynthesis Subcommittee Task Group 223. *Medical Physics*, *41*(9). https://doi.org/10.1118/1.4892600

Sechopoulos I., Ali Elsayed S. M., Badal A., Badano A., Boone J. M., Kyprianou I. S., Mainegra-Hing E.,

McNitt-Gray M. F., McMillan K. L., Rogers D. W. O., Samei Ehsan, T. A. C. (2015). Monte Carlo Reference Data Sets for Imaging Research. The Report of AAPM Task Group 195. In *Medical Physics* (Vol. 42, Issue 195). https://doi.org/10.1118/1.4928676

Tucciariello, R. M., Barca, P., Lamastra, R., Traino, A., & Fantacci, M. (2020). Monte Carlo Methods to evaluate the Mean Glandular Dose in Mammography and Digital Breast Tomosynthesis. In T. B. Hall (Ed.), *Monte Carlo Methods: History and Applications* (pp. 73–110). Nova Science Publishers, Inc.

Tucciariello, R. M., Barca, P., Caramella, D., Lamastra, R., Retico, A., Traino, A., & Fantacci, M. E. (2020). 3D printing materials for physical breast phantoms: Monte Carlo assessment and experimental validation. *BIODEVICES 2020 - 13th Int. Conf. Biomed. Electron. Devices, Proceedings; Part 13th Int. Jt. Conf. Biomed. Eng. Syst. Technol., BIOSTEC 2020*, 254–262. https://doi.org/10.5220/0009162302540262

Tucciariello, R. M., Barca, P., Caramella, D., Lamastra, R., Traino, C., & Fantacci, M. E. (2019). Monte carlo methods for assessment of the mean glandular dose in mammography: Simulations in homogeneous phantoms. *BIOINFORMATICS 2019 - 10th Int. Conf. Bioinforma. Model. Methods Algorithms, Proceedings; Part 12th Int. Jt. Conf. Biomed. Eng. Syst. Technol., BIOSTEC 2019*, 242–249.

Tucciariello, R. M., Barca, P., Lamastra, R., Traino, A., & Fantacci, M. E. (2020). Monte Carlo Methods to Evaluate the Mean Glandular Dose in Mammography and Digital Breast Tomosynthesis. In T. B. Hall (Ed.), *Monte Carlo Methods* (pp. 73–110). Nova Science Publishers, Inc. https://novapublishers.com/shop/monte-carlo-methods-history-and-applications/

Van Engen, R. E., Bosmans, H., Bouwman, R. W., Dance, D. R., Lazzari, P., Marshall, N., Phelan, N., Schopphoven, S., Strudley, C., Thijssen, M. A. O., & Young, K. C. (2018). Protocol for the Quality Control of the Physical and Technical Aspects of Digital Breast Tomosynthesis Systems. *Euref*, *March*, 84.

Wu, X., Gingold, E. L., Barnes, G. T., & Tucker, D. M. (1994). Normalized Average Glandular Dose in Molybdenum target-Rhodium Filter and Rhodium target-Rhodium Filter Mammography. *Radiology*, *193*, 83–89.

Yuuhaa, M. I. W. C., S, L. S., Bidang, P., Lingkungan, D., Amrullah, H., Law, A. O. F., Rahma, S. S., Mutiara, K., Murad, C., Baja, I., Utomo, K. S., Muryani, C., Nugraha, S., Sjafei, I., سيادت سعيد ,بيييييييييييييى ثبْثبْ, นคเรศ รังควัต., Kota, D. I., & Selatan, T. (2018). *World Health Statistics 2018*. https://doi.org/10.20961/ge.v4i1.19180.